Development of a Hall-Effect Thruster with integrated Thrust Vector Control, Concept and Test Results

IEPC-2024-119

Presented at the 38th International Electric Propulsion Conference
Pierre Baudis Convention Center • Toulouse, France
June 23-28, 2024

Willy Stark[1], Oliver Neunzig[2] and Martin Tajmar[3]
Technische Universität Dresden, Dresden, 01069, Germany

While traditional Hall-effect thrusters are known for their high specific impulse and efficiency, they require additional mechanical components to achieve the precise thrust vector control required for orbital maneuvers and attitude corrections. These additional components can impact the overall system performance by increasing weight, volume, complexity, and susceptibility to failure. To address these issues, the Technische Universität Dresden (TUD) has developed an innovative Hall-effect thruster with a segmented anode, the TUD-3D-1. This design allows thrust vector control in all three spatial directions solely by manipulating the ion beam, eliminating the need for additional mechanical components. The paper explains the underlying principles, as well as potential benefits of this advanced thruster technology and presents test results of the prototype.

Nomenclature

B	=	magnetic flux density	m_i	=	ion mass
e	=	elementary charge	P_d	=	discharge power
F	=	thrust	U_d	=	discharge voltage
I_D	=	discharge current	v_{ex}	=	propellant exit velocity
I_{sp}	=	specific impulse	η_a	=	anode efficiency
$\dot{m}$	=	mass flow			

I.Introduction

HALL-effect thrusters (HETs) are widely used as propulsion systems for orbit and attitude control of satellites[1]. These satellites are typically placed in a temporary orbit by launch vehicles and then transferred to their target orbit. To reach this orbit, the satellites need their own propulsion system. Once the satellites reach their target orbit, additional applications arise. Due to atmospheric friction in low Earth orbit, the satellite is constantly slowed down and has to correct its orbit from time to time. A suitable propulsion system is also required to perform evasive maneuvers if there is a risk of collision with another object. To perform such orbit correction maneuvers or attitude control, a propulsion system that can generate thrust forces in all three spatial directions is required.

So far, there have been several ways to use HETs to steer the spacecraft in all three spatial directions. One method involves mechanical gimbals that rotate the thruster within a certain range and change the thrust direction accordingly[2,3]. Another approach uses multiple thrusters that are oriented differently or arranged in clusters to provide multidirectional thrust[4]. In addition, reaction wheels can be used to orient the spacecraft before firing the thrusters to

[1] Research Associate, Institute of Aerospace Engineering, willy.stark@tu-dresden.de
[2] Research Associate, Institute of Aerospace Engineering, oliver.neunzig@tu-dresden.de
[3] Institute Director, Professor and Head of Space Systems Chair, Institute of Aerospace Engineering, martin.tajmar@tu-dresden.de

achieve the desired thrust direction[5]. There have also been efforts to manipulate the magnetic field of the HET to deflect the ion beam and thereby adjust the thrust vector[6]. Each of these solutions requires additional components, adding to the complexity of the system. Mechanical gimbals require significant mechanical parts and additional electrical power, increasing the size and complexity of the system. The use of multiple thrusters also increases the overall complexity, weight, and cost of the system. Reaction wheels, while useful, are another subsystem that must be integrated for effective attitude control and orbital maneuvers. Magnetic field manipulation to steer the ion beam requires additional hardware, further increasing weight and power consumption. All of these methods and technologies increase the complexity, weight, and volume of the propulsion system, resulting in higher costs and increased potential for malfunction.

To address these challenges, Technische Universität Dresden (TUD) is developing a new HET configuration with a segmented anode that eliminates the need for additional mechanical components by controlling the thrust vector solely through ion beam manipulation. This innovative design aims to reduce the weight and volume of the propulsion system while minimizing complexity and susceptibility to failure. This is particularly beneficial for small satellites or CubeSats, which have stringent space and weight constraints.

II.Thrust Vectoring Concept for HET

A. Hall-Effect Thruster Theory

The fundamentals and operation of a HET are well documented in the literature[7]. In a HET, thrust is generated by accelerating ions through an electric field. This thrust is determined by the mass flow rate $\dot{m}$ of the propellant and its exit velocity v_{ex}:

$$F = \dot{m}\, v_{ex} \tag{1}$$

The exit velocity of electrostatically accelerated ions is given as:

$$v_{ex} = \sqrt{\frac{2eU_d}{m_i}} \tag{2}$$

where e is the elementary charge, U_d is the discharge voltage and m_i is the ion mass. Accordingly, increasing the acceleration voltage results in higher thrust. Conventional HETs generate an electric field between the anode at the base of the discharge channel and the electron space charge at the front of the channel, which accelerates the ionized propellant. This produces a uniform thrust vector distribution along the exit plane, resulting in an overall axially directed thrust. To use the ion beam of a HET for steering in different directions, this uniform thrust distribution must be intentionally perturbed. Since the charge e and the ion mass m_i are constants in a given system, the thrust behavior of an HET can only be modified by adjusting the discharge voltage U_d or the mass flow rate $\dot{m}$. Therefore, a new HET design is being developed that allows the application of different local discharge voltages at the anode and non-uniform injection of the propellant.

B. Segmented Anode Concept

Based on previous work[8,9], TUD developed a 500 W HET equipped with a segmented anode for thrust vector control, the TUD-3D-1. It has two coils concentrically arranged around the discharge channel, along with two magnetic screens that deflect the magnetic field to achieve magnetic shielding. An extensive parameter study was performed using COMSOL Multiphysics software to determine optimal values for the axial and radial dimensions of the screens and the coil currents. This geometric setup generates a magnetic flux density peak a few millimeters downstream of the channel exit plane. By adjusting the coil currents, radial peak flux density values between 15 mT and 25 mT can be achieved. Figure 1 shows the magnetic field lines for a representative combination of coil currents.

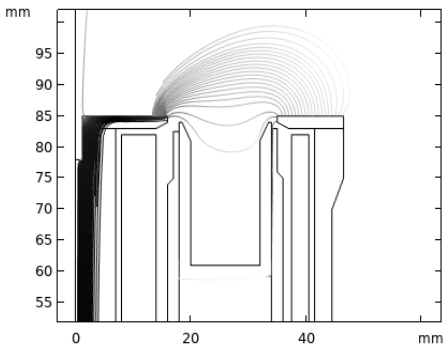

Figure 1 COMSOL Multiphysics plot of the magnetic field lines.

To implement the concept of setting different local discharge voltages, the anode is divided into three separate segments. Each

The 38th International Electric Propulsion Conference, P. Baudis Convention Center, Toulouse, France June 23-28, 2024

segment spans an angle of 114°, with a 6° gap between adjacent segments. By setting different anode potentials on each segment, regions of varying electric field strengths are created within the discharge channel, which should alter the exit velocities of the ions in the azimuthal direction at the exit plane. Figure 2 shows a 3D-model of the thruster with the segmented anode.

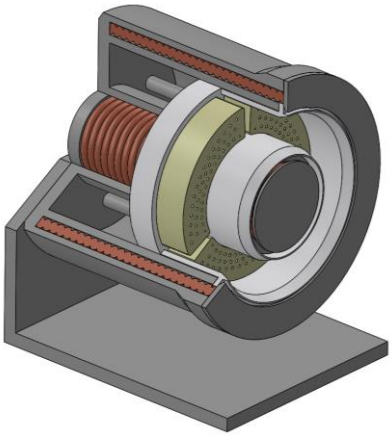

Figure 2 3D-model of the TUD-3D-1 with three anode segments.

Each segment consists of a hollow base and has its own gas supply. The propellant gas flows into the hollow base where it can be uniformly distributed before passing through the porous ceramic cover. The anode disk, located above the cover, contains small holes through which the propellant gas enters the discharge channel. Each anode segment has an independent electrical contact and is electrically isolated from the other segments. Figure 3 Left shows the front view of the TUD-3D-1 with the three anode segments visible in the discharge channel.

This arrangement allows different electrical potentials to be applied to each anode segment, creating an inhomogeneous electric field within the discharge channel. Ions present in the discharge channel are accelerated by the local electric field and generate a corresponding thrust. Therefore, applying different discharge voltages to each anode segment can lead to different accelerations of the ions in the areas of the three anode segments, and thus to different local force vectors. This results in an inhomogeneous force vector distribution over the area of the exit plane of the discharge channel. Such an inhomogeneous force vector distribution causes turning moment around the center of gravity of the HET. By varying the anode potentials, the torque can be controlled and the thruster can be rotated around its pitch and yaw axis. A two-dimensional sketch of the concept is shown in Figure 3 Right.

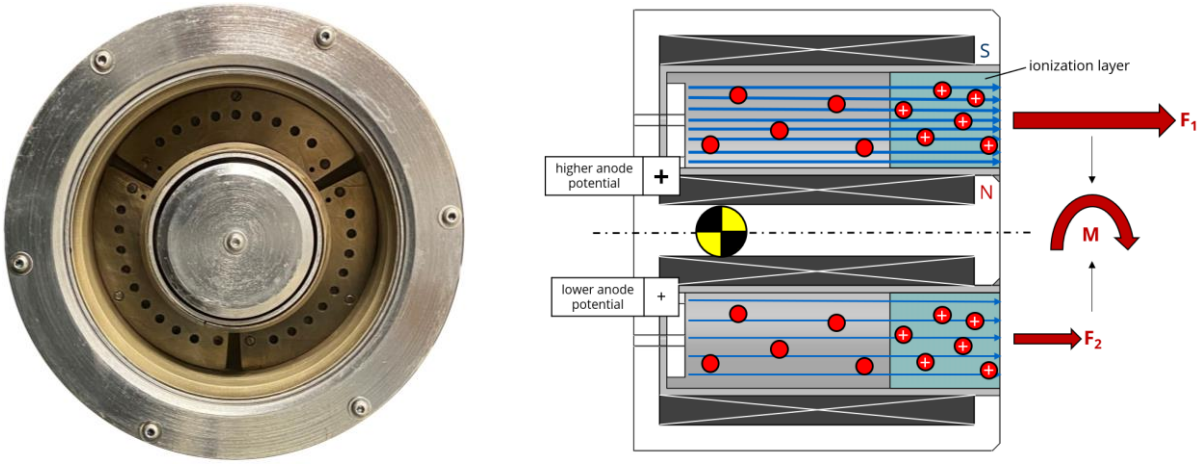

Figure 3 Left: Three anode segments built into the discharge channel of TUD-3D-1. Right: Schematic 2D sketch of the working principle of the HET with different anode potentials.

In Figure 3 Right, the upper anode has a higher potential than the bottom anode. The ions of the propellant gas are accelerated according to the local electric field and produce a thrust F. Due to the higher accelerating voltage of the top anode, the local ions in its vicinity experience a greater acceleration than the local ions of the bottom anode and thus produce a greater thrust. This results in an imbalance of forces that creates a torque around the center of mass.

Since each of the three anode segments has its own gas supply, different mass flow rates can be set for each segment. According to Eq. (1), a higher mass flow rate produces a higher thrust. Changes in the local thrust vector might be possible by a non-uniform propellant injection to the segments. This could support and enhance the effect of the different anode voltages on the local thrust vectors. In other work, it has been shown that a non-uniform propellant flow rate can reduce the discharge oscillation current, but reduces the thrust efficiency of an anode layer type HET[10]. The anode voltage is a crucial factor in the ignition and operating behavior of the thruster. Different anode potentials

could lead to unstable discharges. The TUD-3D-1 underwent detailed characterization to determine performance data and precise testing to investigate the concept of thrust vector control by the segmented anode.

III.Characterization Tests

A. Test Facility

The Institute of Aerospace Engineering of TUD has the infrastructure and equipment for detailed characterization of electric space propulsion systems. The tests can be performed in a large rectangular vacuum chamber (2.5 m long, 1.2 m wide and 1.5 m high). The dimensions of the chamber ensure that interactions of the plasma with the chamber walls are minimized. In addition, there is sufficient space for the installation of the thruster and diagnostics. A cryopump with a nominal pumping rate of 10000 l/s of nitrogen is connected to this chamber, providing a base pressure of less than 1E-7 mbar without mass flow from the thruster or cathode. With additional mass flow through the thruster and cathode, the chamber pressure increased to 5-8E-4 mbar.

The TUD-3D-1 was mounted onto a double pendulum thrust balance developed by Neunzig et al.[11] to measure the thrust during operation. The thrust force from the TUD-3D-1 causes a deflection of the double pendulum balance, which is pivoted by torsion springs of known stiffness. This deflection is measured with a laser interferometer and converted into a corresponding force. The thrust balance has been calibrated in advance with defined forces using a voice coil actuator and can measure thrust forces of up to 50 mN. In smaller measuring ranges, resolutions in the nN range can be achieved. The balance can carry up to 10 kg of additional weight and has two propellant feedthroughs, 16 electrical contacts and 3 thermocouple lines.

The Kaufman & Robinson, Inc. MHC1000 electron source, capable of operating at up to 20 A of emission current, was used for operation with the TUD-3D-1 and mounted on the thrust balance close the thruster. The mass flow through the cathode was 10 sccm of krypton throughout the tests. Figure 4 shows the setup of the TUD-3D-1 and the cathode mounted on the thrust balance.

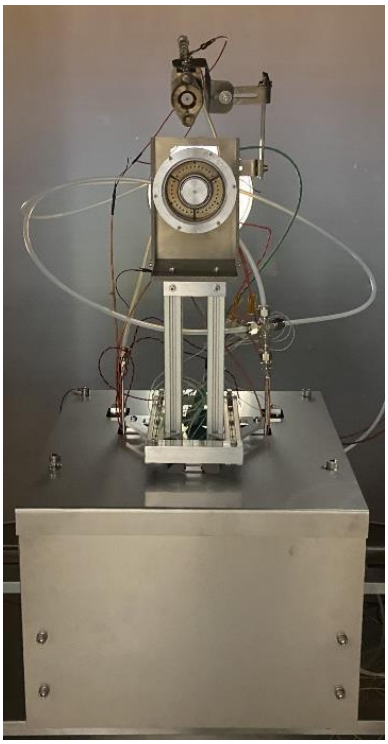

Figure 4 Setup of the TUD-3D-1 mounted on the thrust balance.

B. General Performance

Before investigating the functionality of the segmented anode concept, a general performance characterization of the TUD-3D-1 was performed using krypton as the propellant. Typically, HETs are optimized for xenon, but the use of krypton is gaining significant interest due to its much lower cost compared to xenon. The magnetic flux density at the exit plane was measured in advance and was 23 mT for the subsequent tests. To investigate the general performance of the TUD-3D-1, the three anode segments were electrically connected so that the same voltage could be applied to the entire anode as in conventional HETs. Table 1 shows the performance data when operating at maximum thrust.

The installation of the thruster on the thrust balance lengthens the gas tube path, which also affects the gas line to the anode. Tests without the thrust balance and shortened gas line reduced mass flow to 11 sccm, while other performance data remained similar. This would increase the actual values for I_{sp} and anode efficiency η_a by a factor of about 1.4. Unfortunately, these measurements cannot be used to calculate I_{sp} and anode efficiency because no thrust could be measured without a thrust balance. It is possible that there was a small leak in the gas line during the thrust balance measurements, causing a higher propellant consumption.

Table 1 Performance Data of the TUD-3D-1 for highest thrust.

	TUD-3D-1
P_d	330 W
U_d	275 V
I_d	1.2 A
B	23 mT
$\dot{m}$	0.97 mg/s (15.5 sccm Kr)
F	11.7 mN
I_{sp}	1235 s
η_a	21.5 %

C. Segmented Anode Tests

After determining the general performance data of the TUD-3D-1, the concept of the segmented anode was investigated to see if stable operation with different anode voltages was possible. The anode segments were electrically isolated from each other and each segment was powered by an independent power supply. The tests were conducted in such a way that ignition was performed with the same voltages at each anode segment as in normal operation to establish a stable operating point. The TUD-3D-1 was operated in current-controlled mode, with the current at each anode limited to 0.4 A, for a total of 1.2 A. Voltage limits were then set at the active discharge voltage for each anode segment, causing the thruster to operate in voltage-controlled mode, and the current limits were removed. Thus, each anode segment adjusted an individually required discharge current. For the purpose of the study, the voltage limit of one of the anode segments was then gradually reduced and later increased again. Figure 6 shows an example of such a measurement and Figure 5 shows the naming of the anode segments.

Figure 5 Front view of the TUD-3D-1.

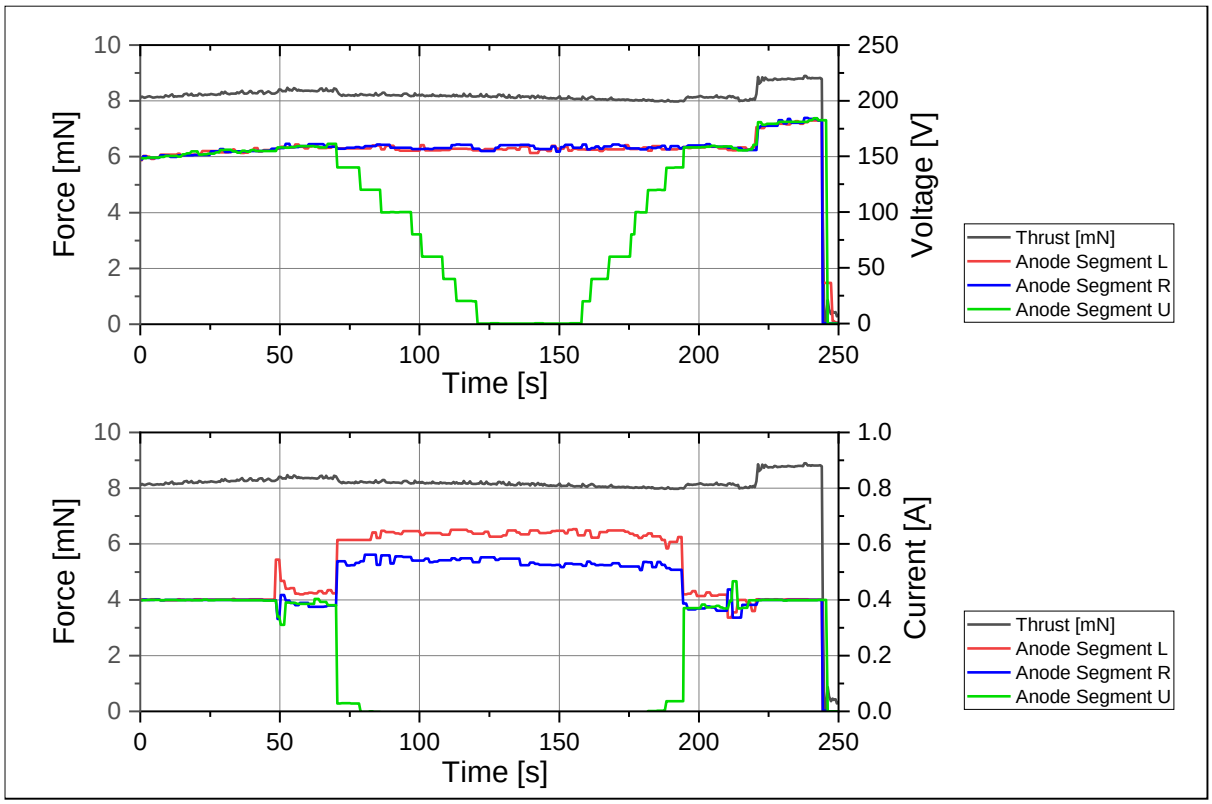

Figure 6 Voltage and current characteristics of the TUD-3D-1 with one down-regulated anode segment.

In the test presented, the TUD-3D-1 was operated at a power of approximately 200 W and a gas flow of 17.5 sccm of krypton. Previous tests have shown that this operating point remains stable even when some parameters are changed and is therefore suitable for the segmented anode test. For the first 50 seconds of the measurement, the TUD-3D-1 is operated in a current-controlled mode. Then, the voltage limits were set to 160 V and the current limits were removed, so that the thruster operated in voltage-controlled mode. The voltage at the upper anode segment was then gradually reduced to 0 V in 20 V steps. It can be observed that as soon as the voltage of the upper anode is reduced slightly, the corresponding anode current suddenly drops to 0 A, while the left and right anode segments compensate for this and their combined anode current increases to 1.2 A. Finally, the voltage on the upper anode segment was gradually increased to 160 V and the current and voltage values returned to their original state. The thruster operated in a stable state and generated a steady thrust throughout the whole test run, even though one anode segment was temporarily set to 0 V. When the voltage on one segment was reduced, the total thrust also decreased slightly by about 0.2 mN. This

could indeed be due to the desired inhomogeneous force vector distribution at the exit plane. Returning the voltage at the upper anode segment to its original value of 160 V also results in a slight increase in total thrust.

In the next test run, the voltage on two of the three anode segments of the TUD-3D-1 was to be reduced. Again, ignition was performed with the same voltages at each anode segment as in normal operation to establish a stable operating point. The thruster was operated in current-controlled mode, with the current at each anode limited to 0.4 A, for a total of 1.2 A. Voltage limits were then set at the active discharge voltage for each anode segment, causing the thruster to operate in voltage-controlled mode, and the current limits were removed. Thus, each anode segment adjusted an individually required discharge current. The voltage limits of two anode segments were then gradually reduced and later increased again.

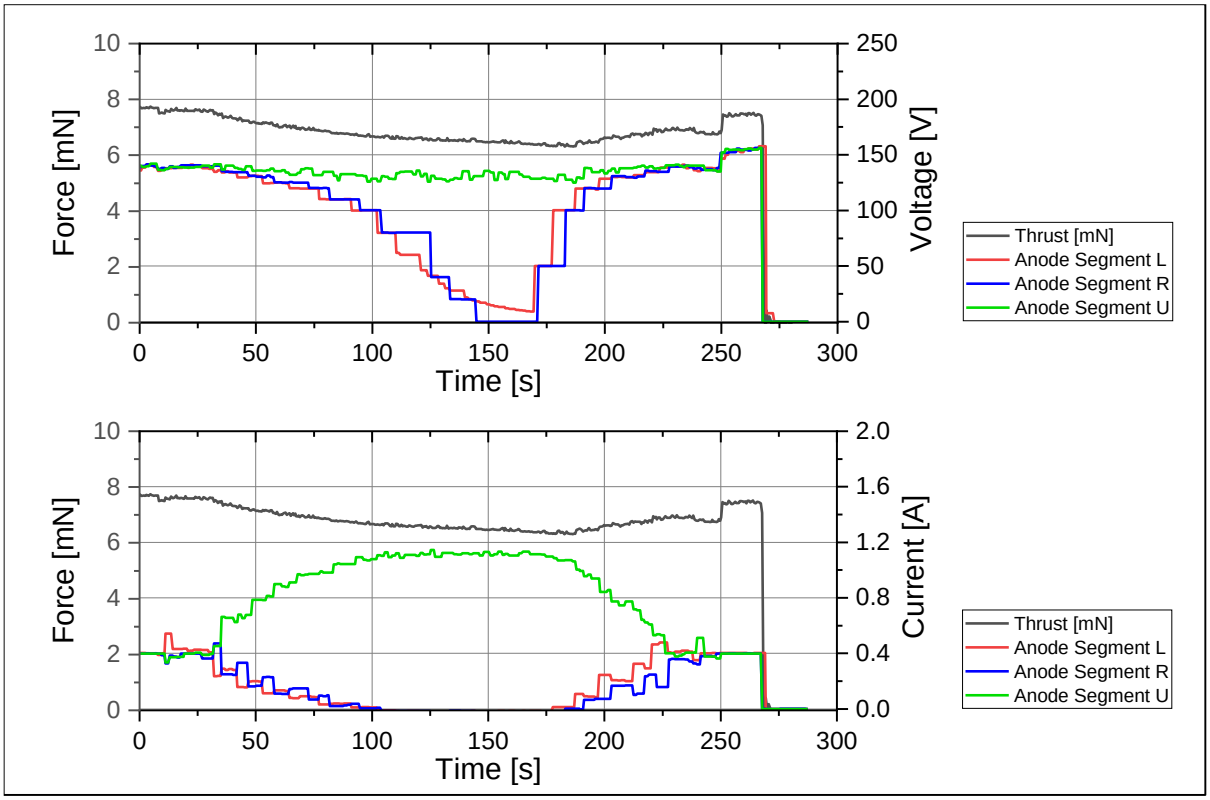

Figure 7 Voltage and current characteristics of the TUD-3D-1 with two down-regulated anode segments.

This test was performed with power of 170 W and a gas flow of 18 sccm of krypton. Again, the thruster was ignited in the conventional manner and a stable operating point was established, running the TUD-3D-1 is in current-controlled mode. Then the voltage limits were set to 140 V and the current limits removed, so that the thruster operated in voltage-controlled mode. The voltages at the left and right anode segments were then gradually reduced, first in 5 V steps and later in larger steps, until 0 V was commanded by the power supplies. The voltage at the right anode segment actually dropped to 0 V, while the voltage at the left anode segment dropped only to 10 V. It can be observed that as the voltages of the two anode segments gradually decreased, the associated current also decreased, while the current of the remaining anode segment steadily increased. When the voltage at the left and right anode segments dropped below 100 V, the corresponding current dropped to 0 A, while the current at the upper anode segment increased to 1.1 A, compensating for the other two segments. Even in this state with two anode segments at 0 V, the thruster continued to operate stably. Finally, the voltages on the left and right anode segments were gradually increased to 140 V and the current and voltage values returned to their original state. The thruster generated a steady thrust throughout the whole test run, starting at 7.8 mN. The total thrust decreased as the voltage at the two anode segments were gradually reduced, still generating 6.4 mN when both segments were set to 0 V. Steadily increasing the voltages at the left and right anode segments to their original values of 140 V also steadily increased the total thrust. This is an indication that the thrust vectors may have shifted in different directions, but the thrust balance can only measure thrust in the axial direction.

IV. 2D-Mapping of the Ion Beam

A. Planar Probe Array Setup

To further investigate the functionality of the thrust vector control, an ion beam mapping diagnostic was developed. It should be used to measure the local ion current density and to display it in the form of a 2D map. For this purpose, an array of 9x9 planar probes (81 in total) was manufactured and could be placed in the vacuum chamber. The array frame consists of adjustable rails to vary the distance between the probes, and the probes themselves can be moved along these rails to allow different positioning. The primary function of the planar probe array is to visualize the ion beam based on the local ion current density and show changes in its distribution, rather than to measure the exact ion current density. For this reason, and because of the large number of total probes, a simple modular probe design has been developed with an emphasis on rapid production of the individual parts. The design is based on a guideline for planar probes[12].

The main body of the probes is 3D printed PC with a 55 mm diameter collector disk made of stainless-steel glued to its front. The collector is surrounded by a stainless-steel guard ring, and the two are electrically isolated. There is a BNC connector for the collector on the back of the unit, as well as a bracket for mounting to the array rails. The collectors are connected to a power supply via their own measuring resistor, while the guard rings are connected directly to the power supply. An expanded Labjack T7 with 84 analog input channels measures the voltage drop in parallel with the individual measuring resistors, allowing the current from all 81 planar probes to be read simultaneously. Figure 8 shows an image of such a planar probe on the left and the schematic circuit diagram is shown

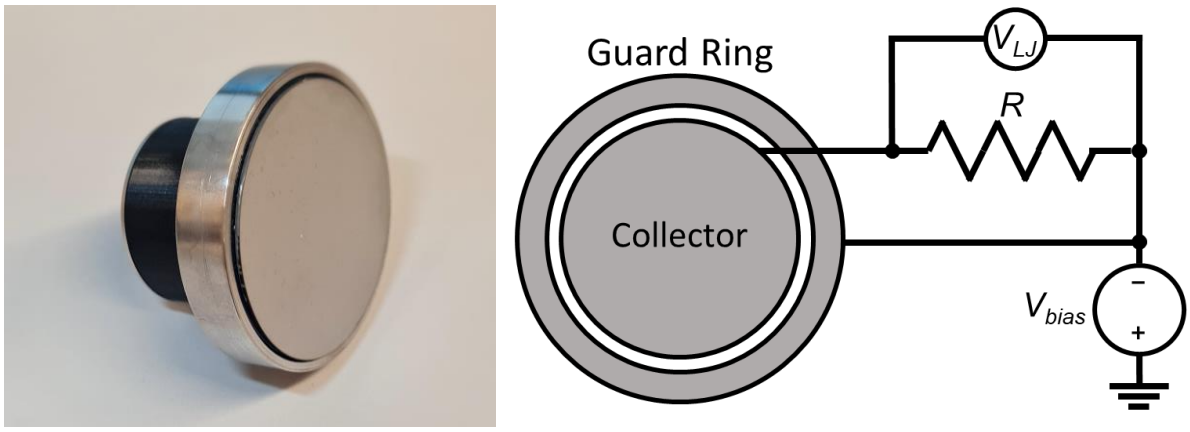

Figure 8 Left: Planar Probe.
Right: Schematic circuit diagram for the planar probe setup.

on the right.

B. Planar Probe Array Measurements

The planar probe array was placed in the vacuum chamber and the TUD-3D-1 was aligned centrally at a distance of 160 cm. The probes were spaced 75 mm apart to provide a very compact resolution and set to -10 V to attract ions only and measure the local ion current. The tests were performed without the thrust balance, so no thrust could be measured. Unfortunately, only the results for operation under normal performance parameters, i.e. with the same voltages on all three anode segments, can be shown. Not enough data could yet be collected for measurements at different anode voltages. The performance data of the TUD-3D-1 for this measurement is shown in Table 2. Figure 9 shows the setup of the planar probe array and the thruster in the vacuum chamber on the left, and the 2D mapping of the ion current on the right. The identification of each probe is based on a coordinate system similar to the game *Battleship*. The rails are labeled with letters from *A* to *I* starting from the top, and the probes on that rail are labeled with numbers from *1* to *9* starting from the left.

Table 2 Performance Data for Planar Probe Array Measurements.

	TUD-3D-1
P_d	342 W
U_d	285 V
I_d	1.2 A
B	23 mT
$\dot{m}$	0.75 mg/s (12 sccm Kr)

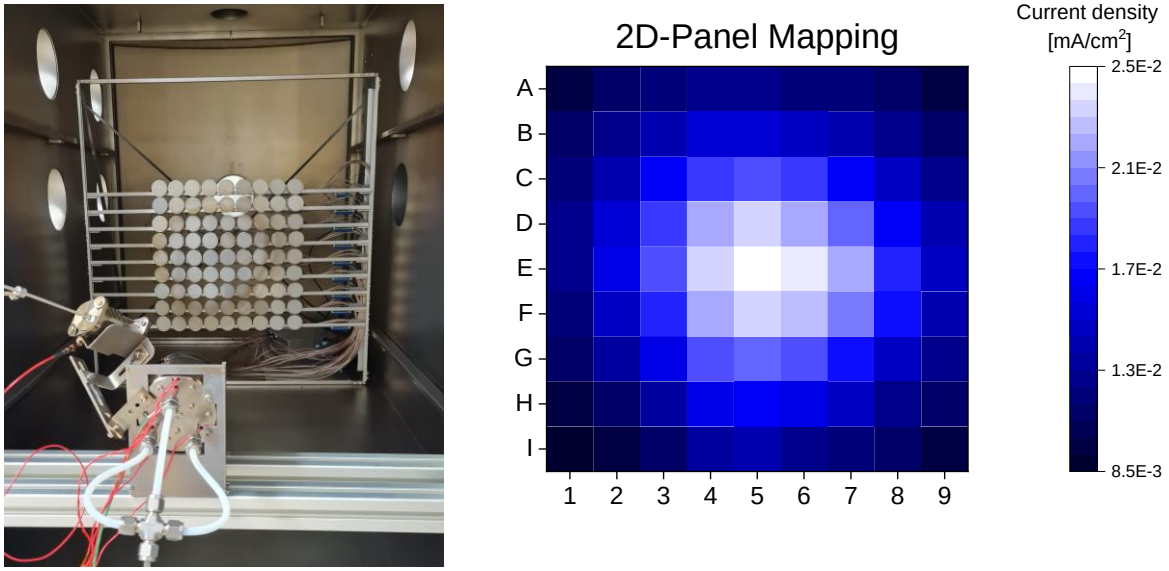

Figure 9 Left: Setup with Planar Probe Array and TUD-3D-1 in vacuum chamber. Right: Mapping of the current density by the Planar Probe Array.

At a distance of 160 cm from the thruster, the highest ion current density was measured in the center (E5), reaching 2.5E-2 mA/cm^2, while the lowest ion current density was found in the corners of the planar probe array (A1, A9, I1 and I9), reaching 8.5E-3 mA/cm^2. Such an ion current distribution is typical for a HET with the highest ion current density in the center and decreasing toward the edge. In the future, this method should also show changes in the ion current distribution when operating with different voltages at the anode segments, thus proving the functionality of the thrust vector control of the TUD-3D-1.

V.Conclusion

Based on the concept of integrated thrust vector control by different anode potentials, a HET with a segmented anode, the TUD-3D-1, has been developed and first test results have been collected. First, the general performance data of the thruster were recorded and stable operating points were determined before the functionality of the segmented anode was investigated. Thrust forces of up to 11.7 mN were measured at a power of 330 W and an I_{sp} of 1235 s. It should be noted that the gas flow to the thruster was increased during this measurement due to the longer gas lines and potential leakage on the thrust balance compared to a measurement without the thrust balance. The additional gas flow degrades the I_{sp}, so the actual I_{sp} is likely to be higher. Furthermore, it has been shown that the voltages on the individual anode segments can be reduced during operation without the thruster becoming unstable. Even if two of the three segments are set to 0 V, stable operation is guaranteed by the one remaining segment. This is a basic requirement for the implementation of the presented concept of an integrated thrust vector control for the HET.

In addition, a planar probe array was developed for 2D visualization of the ion current density in the far field of the thruster. An ion current density distribution was determined and displayed for normal operation of the TUD-3D-1. In the future, this method should also be able to show possible deflection or asymmetric distribution as a result of segmented anode operation.

The results so far are promising and TUD is continuously improving the thruster and diagnostics to realize the HET with integrated thrust vector control for orbit and attitude control. TUD is currently developing a thrust balance setup consisting of a double pendulum balance with an integrated gimbal balance to determine the total thrust and to measure the tilting moments that may be generated by the thruster. Together with the planar probe array measurements, this will be the ultimate test to prove whether or not the segmented anode HET concept can provide thrust vector control.

Acknowledgments

We gratefully acknowledge funding by the German Aerospace Center DLR (50RS2103).

References

1. Lev, D. *et al.* The Technological and Commercial Expansion of Electric Propulsion in the Past 24 Years. *The 35th International Electric Propulsion Conference* IEPC-2017-242 (2017).
2. Biron, J. *et al*. The Thruster Module Assembly (Hall Effect Thruster) design, qualification and flight. *Proceedings of the International Electric Propulsion Conference 2005 (IEPC05)* **2005**, 1–7 (2005).
3. Lorand, A., Duchemin, O. B. & Cornu, N. Next Generation of Thruster Module Assembly (TMA-NG). *32nd International Electric Propulsion Conference* IEPC-2011-201 (2011).
4. Duchemin, O. Multi-Channel Hall-Effect Thrusters: Mission Applications and Architecture Trade-Offs. *Assembly* 1–15 (2007).
5. Wertz, J. R. *Space Mission Analysis and Design*. (Microcosm Press, Hawthorne, Calif., 2007).
6. Duchemin, O. *et al.* Development of a Prototype Thrust Steering Device for Hall-Effect Thrusters. *Proceedings of the 4th International Spacecraft Propulsion Conference* (2004).
7. Goebel, D. M. & Katz, I. Fundamentals of Electric Propulsion: Ion and Hall Thrusters. *Fundamentals of Electric Propulsion: Ion and Hall Thrusters* 1–507 (2008) doi:10.1002/9780470436448.
8. Gondol, N., Drobny, C., Neunzig, O. & Tajmar, M. Development and Characterization of a Miniature Hall-Effect Thruster using Permanent Magnets. *36th International Electric Propulsion Conference, University of Vienna, Austria, September 15-20* 1–13 (2019).
9. Stark, W., Gondol, N. & Tajmar, M. Concept and design of a hall-effect thruster with integrated thrust vector control. *Journal of Electric Propulsion* **1**, 21 (2022).
10. Fukushima, Y., Yokota, S., Komurasaki, K. & Arakawa, Y. Influence of Azimuthally Nonuniform Propellant Flow Rate on Thrust Vector and Discharge Current Oscillation in a Hall Thruster. *Transactions of the Japan Society for Aeronautical and Space Sciences, Space Technology Japan* **7**, 41–45 (2009).
11. Neunzig, O. & Tajmar, M. Verification of a Novel Collector-Thrust Measurement using Low-Power Hall-Effect Thruster. in *9th Space Propulsion Conference* (SP2024_318, Glasgow, Scotland, 2024).
12. Brown, D., Walker, M., Szabo, J., Huang, W. & Foster, J. Recommended Practice for Use of Faraday Probes in Electric Propulsion Testing. *J Propuls Power* **33**, (2016).